A 500 MHz – 2.7 GHz 8-Path Weaver Downconverter with Harmonic Rejection and Embedded Filtering

Remko E. Struiksma, Eric A.M. Klumperink, Bram Nauta and Frank E. van Vliet
IC Design Group, University of Twente, Enschede, The Netherlands

***Abstract*—This paper describes a combination of a Weaver mixer and an N-path filter for a superheterodyne receiver with a reconfigurable frequency plan. It uses an N-path topology driven with two different frequencies, effectively realizing a frequency shift together with band-pass filtering. To reduce transfers via harmonics other than the fundamental, a harmonic rejection scheme is used. A 28 nm FDSOI CMOS implementation with 30 dB harmonic rejection and an out-of-band IIP3 of >20 dBm is demonstrated.**

***Keywords*—Receiver, mixer, N-path filter, image rejection, harmonic rejection, frequency conversion, superheterodyne receiver**

I. Introduction

Many existing receiver systems (in radar [1, Sec. 6.1] and communication [2, Sec. 13.1]) operate on the superheterodyne principle, in which the RF input signal is mixed with that of a local oscillator (LO) to a non-zero intermediate frequency (IF).

A conventional mixer has two input frequencies, above and below the LO frequency, which convert to the same IF frequency. One way to reject the unused response, called image, is to use a Weaver architecture [3] as shown in fig. 1. In this architecture all 90° phase shifts can be introduced in the LO path by using frequency dividers, which operate over a much wider frequency range than the hybrids, all-pass or sequence asymmetric polyphase filters used in a Hartley architecture [4]. Having the freedom to choose the IF offers the flexibility to change the frequency plan based on the interferer scenario.

Another way to describe fig. 1 is a narrow band filter of which the centre frequency is determined by the modulating frequency [5]. In such an N-path filter all modulators normally use the same frequency f_0, shifting the transfer of the low-pass filter to a centre frequency of f_0, while essentially keeping the same shape. With different modulating frequencies this filtering is maintained but the response is at a different frequency than the input. However the use of a second frequency also means that unwanted translations via various combination of harmonics can occur, especially if hard-switching mixers are used. This paper introduces a systematic way to reduce these unwanted folding products.

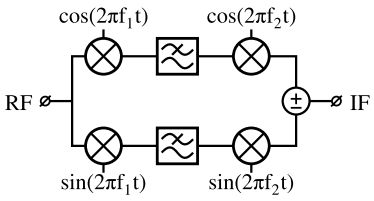

Fig. 1. Weaver mixer ($f_1 \neq f_2$) or N-path filter ($f_1 = f_2$).

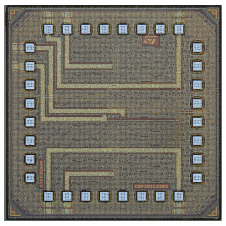

Fig. 2. Die photo

II. Top level description

To achieve high linearity and low flicker noise (important because of the intermediate down-conversion to baseband), the mixers and filters shown in fig. 1 should be passive. A simplified top-level schematic of the complete design is shown in fig. 3. It consists of the main N-path Weaver mixer followed by an amplifying stage, these are described in the next section. The upper part is a translational feedback-loop [6], intended to provide in-band matching. There are two divide-by-four frequency dividers which generate two 8-phase 1/8 duty cycle pulse trains, one at f_1 and one at f_2, which drive the mixers. Finally there are four output buffers to drive the 50 Ω measurement equipment. The in- and outputs are differential, but single-ended connections were used in all measurements except for linearity and noise, with the other terminal terminated in 50 Ω.

III. Principle of operation

In a system with two mixing stages frequency translations via any harmonic combination of the fundamentals $\Delta f = k \cdot f_1 - l \cdot f_2$ can in principle occur, while only one of those is desired. By using an N-path approach [7], frequency translations via different harmonics ($k \bmod N \neq l \bmod N$) can be eliminated. Fig. 4 shows one out of the eight paths, the others are identical except for a rotation in their clock-phases ($0 \rightarrow 1$, $1 \rightarrow 2$, etc). The signal is first downconverted via the switches at the left, then filtered by the RC low-pass filter formed by the source resistance R_S and the capacitor C. The bandwidth of this filter should be much lower than the switching frequency. Subsequently the signal is upconverted via the switches at the right to the desired IF frequency. Because of the rotation in clock phases only one path is connected to each IF phase at a time, and the contributions from the N paths are summed by interleaving. The phase of each contribution depends on combination of harmonics, and as illustrated by figure 5 for $k \bmod N \neq l \bmod N$ they add-up in anti-phase.

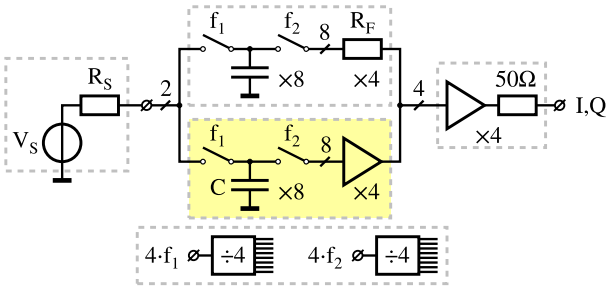

Fig. 3. Conceptual top level schematic. The highlighted core consists of eight switched capacitor sections of which one is shown fig. 4, and four amplifiers of which two are shown in fig. 6.

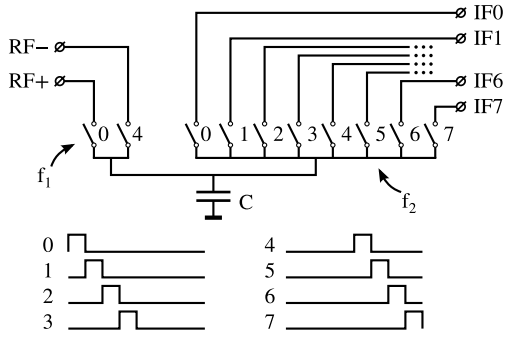

Fig. 4. One out of 8 paths, others identical except clock phase.

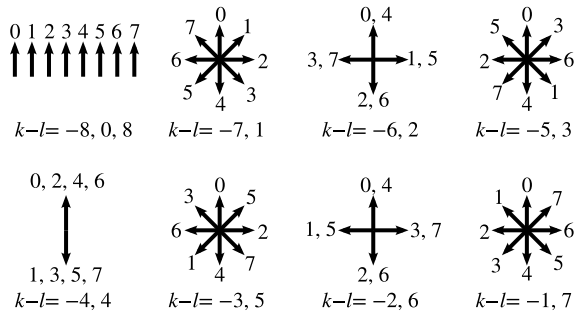

Fig. 5. Contributions to a single IF phase for different harmonic combinations (k,l), the annotated numbers refer to the contributing path.

The remaining translations not only include the wanted transfer $k = l = 1$, but also transfers via the same higher harmonic (modulo N) at the first and second switching stage, as shown by the stars and crosses in fig. 8. These can be eliminated by a sine/cosine weighted addition at IF [8] as shown in fig. 6. By making the direction of rotation for one of the clocks selectable the downconverter can switch between low- and high-side injection (fig. 7), allowing the frequency-plan to be adapted based on the interferer scenario. If in addition quadrature outputs are formed, those translations which give an opposite phase sequence at IF with respect to the wanted translation (which includes the secondary image) may be rejected in a later stage.

The uncancelled sidebands which convert to f_2, when using

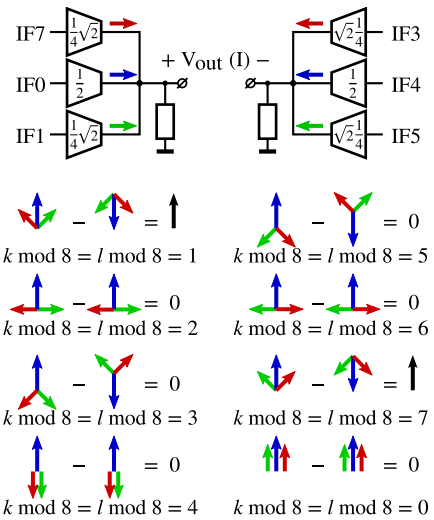

Fig. 6. Harmonic cancellation by weighted addition at IF.

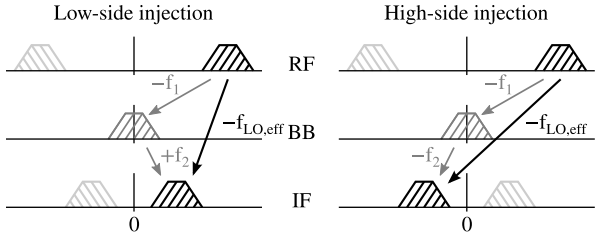

Fig. 7. Intended frequency translations, represented by complex signals.

low-side injection, are at

$$f_{RF} = (p+1)f_1 + qf_2 \quad \text{and} \quad f_{RF} = (p-1)f_1 + (2+q)f_2$$

And when using high-side injection they are at

$$f_{RF} = (p+1)f_1 - qf_2 \quad \text{and} \quad f_{RF} = (p-1)f_1 - (2+q)f_2$$

with $p = 0, N, 2N, \ldots$ and $q = \ldots, -2N, -N, 0, N, 2N, \ldots$. As shown by the dots and triangles in fig. 8 these, apart from the secondary image at $f_1 \pm 2f_2$, are considerably attenuated by the low-pass filter. The strongest folding products at $(1 \pm N)f_1$ are far way from the wanted band and may thus be reduced by a pre-filter.

In a dual conversion system there also exist two mirror frequencies: the primary and secondary image. The primary image is (in the absence of amplitude and phase mismatches) completely suppressed, the secondary image is only partially suppressed due to the finite suppression of the N-path filter. With a quadrature output it can be further suppressed because its phase rotation is opposite to that of wanted sideband. In this system the primary image is a 'self image', i.e. it lays in the pass-band just like the wanted signal but at the other side of the centre frequency, so it is located at $2f_1 - f_{RF}$. The secondary image is located at $f_1 \pm 2f_{IF}$, which may be above or below the wanted RF frequency, depending whether high-side or low-side injection is used respectively.

IV. Measurement Results

The design was implemented in 28 nm FDSOI CMOS, a photograph of the die is shown in fig. 2. The size of the chip is 585 × 585 µm (excluding the padring), the majority of the area is consumed by the baseband MOM-capacitors.

A. Image rejection

The transfer function and image rejection were measured using an input centre frequency of $f_1 = 1800$ MHz, and output centre frequency of $f_2 = 150$ MHz. Table I list the frequency ranges of the wanted transfer (TF), the primary image (PI), the secondary image (SI), and the (absolute) IF frequencies to which they translate, for both injection settings. Fig. 9 shows the measured images and wanted transfers as function of the output frequency, it should be noted that these correspond to different input frequencies. In both injection settings the bandwidth is approx. 7 MHz, and the image rejection for both images is approx. 35 dB.

TABLE I. Frequencies used in measurement.

	Low-side injection		High-side injection	
	RF [MHz]	IF [MHz]	RF [MHz]	IF [MHz]
TF	1750-1850	100-200	1750-1850	200-100
PI	1850-1750	100-200	1850-1750	200-100
SI	1550-1450	100-200	2150-2050	200-100

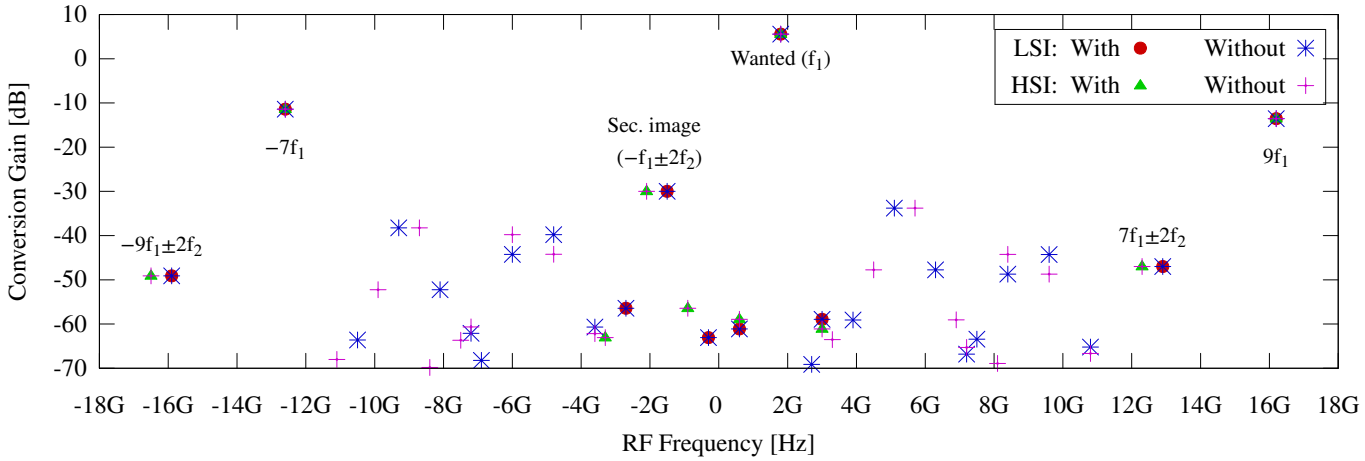

Fig. 8. Simulated folding (using ideal components, BW=10 MHz, f_1=1800 MHz, f_2=150 MHz), with and without the weighted addition at IF.

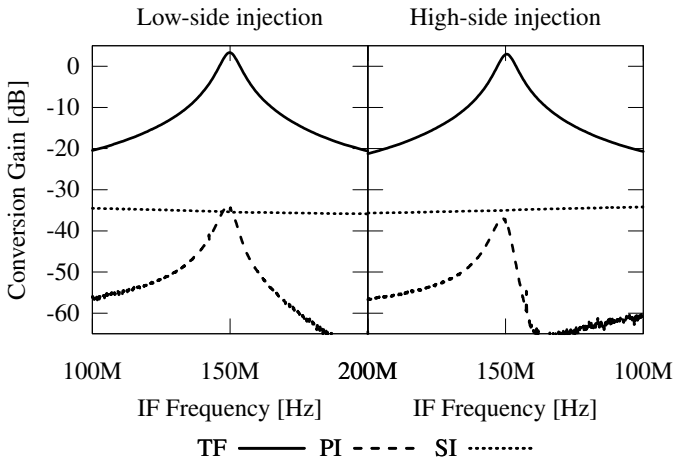

Fig. 9. Measured transfer (TF) and its images (PI, SI).

B. Harmonic rejection

The combination of 1800 MHz and 150 MHz gives a beat frequency of 150 MHz, so frequency translations by any multiple of this can occur. The folding may occur from 'positive' or 'negative' RF frequencies, in one case the output spectrum is mirrored with respect to the input spectrum. By applying a small frequency offset to the input this frequency flip can be detected. Fig. 10 shows the measured transfer to a fixed IF of 150 MHz (with a ±100 kHz offset), where the input frequency is swept with increments of 150 MHz.

It shows that the dominant unwanted folding product is the seventh harmonic ($7f_1$), as is to be expected for an 8-phase system. Then there is a direct feedthrough at ±150 MHz, which is because the measurement was performed single-ended. At 5.4 GHz there is folding from the third harmonic and at 9 GHz from the fifth harmonic. These are assumed to be due to the phase mismatches stemming from using both edges of the input clock in a divide-by-four frequency divider to generate 8 clock phases. Next at approximately the same level there are the images, which were shown in more detail in fig. 9, and folding from $2f_1$, $2f_1 \pm f_2$, $-2f_1$, $-2f_1 \pm f_2$ and $-2f_1 \pm 3f_2$. All other components are more than 40 dB below the wanted transfer.

C. Further results

To characterise the linearity a two-tone test was performed. The out-of-band IIP2 was measured by sweeping the power of two tones, one at 1879 MHz and the other at 1880 MHz. These give a second order intermodulation product at 1 MHz which falls in the pass-band of the low-pass filter. The out-of-band IIP3 was measured with tones at 1840 MHz and 1879 MHz, this gives a third order intermodulation product in the wanted band at 1801 MHz. Both products show up at the output at 151 MHz when using low-side injection. The IM2 and IM3 products together with an in-band fundamental tone are shown in fig. 11, these curves extrapolate to an IIP2 of 59 dBm and an IIP3 of 23 dBm respectively.

The RF tuning range was characterised by sweeping the RF input frequency along with f_1, while keeping f_2 and thus the IF frequency fixed at 150 MHz, and measuring the conversion gain. Fig. 12 shows that the maximum frequency is 2.7 GHz, beyond which the clock divider stops working. Similarly the IF tuning range was characterised by sweeping f_2 while keeping the RF at 1800 MHz. Fig. 12 shows a gradual roll-off of conversion gain with increasing IF, which is assumed to be caused by insufficient on-chip decoupling.

The noise figure measured near the centre frequency is 10 dB, which is on the high side (at least in part) due to some extra series resistance in the layout.

The chip is powered from a 1 Volt supply, consuming 13 mW of static power for the inverter-based amplifiers and output buffers, 10 mW for the input clock buffers (differential pairs), plus 12.6 mW/GHz of IF and 7.2 mW/GHz of RF.

D. Comparison

Table II lists the main measurement results, together with those of a previous superheterodyne receiver incorporating N-path filtering [9]. Comparing them shows that this work compares favourably in linearity (IIP3) due to the passive filtering at the input and unfavourably in noise. The latter is an issue with this specific chip (too much resistance in the layout), theoretically much lower noise figures are possible for passive mixers [10]. Thanks to the cancellation introduced in section III the harmonic rejection is substantially better than the 17 dB reported in [9], though there is definitely room for improvement.

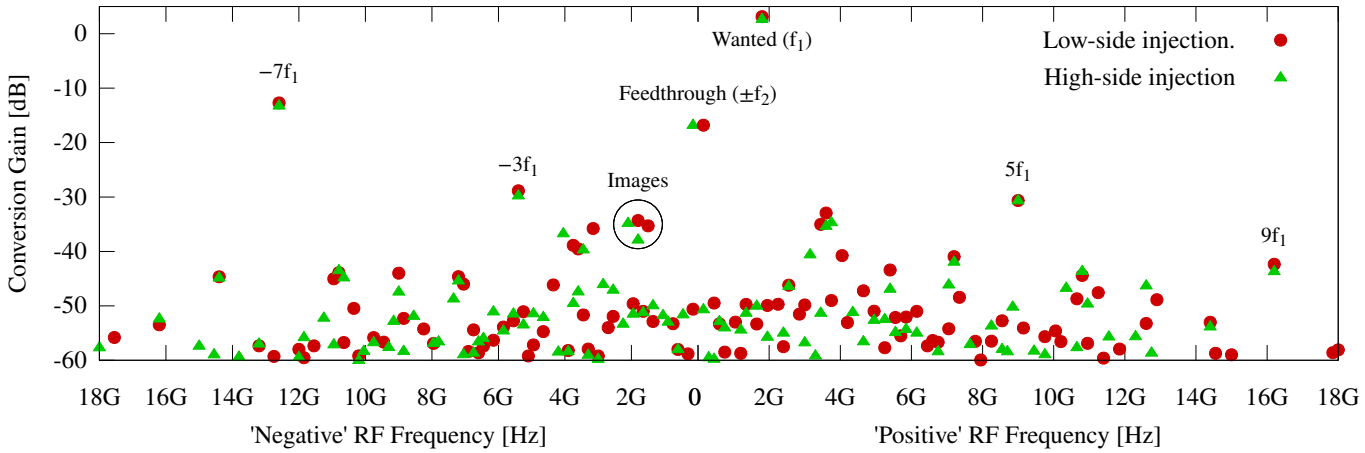

Fig. 10. Measured folding in both injection settings, measurement was performed single-ended.

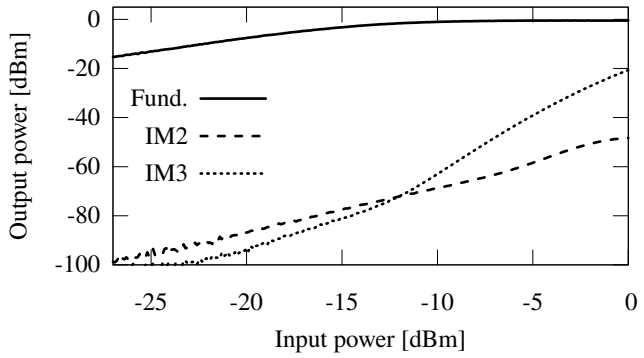

Fig. 11. Measured intermodulation and in-band fundamental.

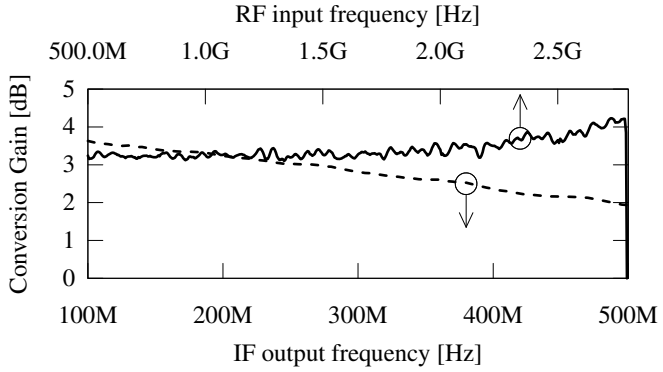

Fig. 12. Measured conversion gain vs frequency.

V. Conclusion

A combination of an N-path filter and a Weaver mixer in CMOS was demonstrated. In which first the contributions of the N paths are added to form N IF phases, which are then combined so that most of the harmonic translations are cancelled. By switching between low- and high-side injection and/or changing the IF frequency the frequency-plan can be adapted, moving some remaining weak spots, based on the interferer scenario.

TABLE II. Measurement results & comparison.

Parameter	This work	Mirzaei et al. [9]
RF freq. [GHz]	0.5 - 2.7	1.8 - 2.0
IF freq. [MHz]	100 - 500	110
Bandwidth [MHz]	7	4
Secondary image rej. [dB]	35	45
Harmonic rej. [dB]	30	17
IIP3 [dBm]	23	−6.3
NF [dB]	10	5.3
Power consumption [mW]	28 - 48	?

Acknowledgement

This research is conducted as part of the STARS project (www.starsproject.nl). The authors also wish to thank ST Microelectronics for silicon donation, CMP for assistance, and Gerard Wienk and Henk de Vries for their support.

References

[1] M. I. Skolnik, *Radar Handbook, Third Edition*. McGraw-Hill, 2008.

[2] T. H. Lee, *The Design of CMOS Radio-Frequency Integrated Circuits, Second Edition*. Cambridge University Press, 2004.

[3] D. K. Weaver, "A third method of generation and detection of single-sideband signals," *Proc. IRE*, vol. 44, no. 12, pp. 1703–1705, Dec 1956.

[4] R. V. L. Hartley, "Modulation system," Patent US 1 666 206, Apr, 1928.

[5] N. F. Barber, "Narrow band-pass filter using modulation," *Wireless Engineer*, vol. 24, pp. 132–134, 1947.

[6] X. He and H. Kundur, "A compact SAW-less multiband WCDMA/GPS receiver front-end with translational loop for input matching," in *IEEE Int. Solid-State Circuits Conf. Dig. Tech. Papers*, Feb 2011, pp. 372–374.

[7] L. E. Franks and I. W. Sandberg, "An alternative approach to the realization of network transfer functions: The N-path filter," *Bell Syst. Tech. J.*, vol. 39, no. 5, pp. 1321–1350, 1960.

[8] J. A. Weldon *et al.*, "A 1.75-Ghz highly integrated narrow-band CMOS transmitter with harmonic-rejection mixers," *IEEE J. Solid-State Circuits*, vol. 36, no. 12, pp. 2003–2015, Dec 2001.

[9] A. Mirzaei, H. Darabi, and D. Murphy, "A low-power process-scalable super-heterodyne receiver with integrated high-Q filters," *IEEE J. Solid-State Circuits*, vol. 46, no. 12, pp. 2920–2932, Dec 2011.

[10] M. C. M. Soer *et al.*, "Unified frequency-domain analysis of switched-series-RC passive mixers and samplers," *IEEE Trans. Circuits Syst. I*, vol. 57, no. 10, pp. 2618–2631, Oct 2010.